# Development of a test apparatus for thermal conductivity measurements of insulation materials with adsorbed nitrogen between 20 and 77 K

**J N Jessop, J W Leachman, K I Matveev**

Hydrogen Properties for Energy Research (HYPER) Center, School of Mechanical and Materials Engineering, Washington State University, Pullman, WA 99164-2920 USA

Email: jacob.leachman@wsu.edu

**Abstract.** Understanding the effective thermal conductivity of insulations utilized in vacuum-jacketed liquid hydrogen vessels is critical to predicting heat leak and boil-off characteristics. More specifically, the ability to predict the transient heat flux during a loss of vacuum event is a critical metric that will impact the design of safety systems and hold time of these tanks. There is a lack of measurements at liquid hydrogen boundary temperatures due to the majority of insulation measurements occurring at liquid nitrogen cold boundary temperatures (77 K and above). Boil-off calorimetry has been a typical method for measuring thermal conductivities but proves challenging for liquid hydrogen temperatures (20 K). In this study, a cryogenic refrigerator enables thermal conductivity measurements of three common insulations (glass microbubbles, aerogel, and multi-layer insulation) with an accuracy better than $\pm 1$ mW/m-K at liquid hydrogen boundary temperatures. Comparisons are made to prior measurements. Additionally, the experiment is capable of uniformly introducing gas in the insulation space, simulating a vacuum failure. Transient heat fluxes can be determined from these experiments and utilized to design safety systems.

## 1. Introduction

Vacuum insulated storage vessels are among the most utilized storage modes for cryogenic fluids due to low parasitic heat leak[1]. Filler materials such as glass microbubbles, aerogel, and MLI can be added to the vacuum space to further reduce heat leak. The performance of these filler materials is determined by measuring the effective thermal conductivities, which vary with boundary temperatures. Aerogel, Glass Microbubbles, and Multi-Layer Insulation (MLI) have all been thoroughly characterized with a liquid nitrogen cold boundary (77 K) via boil-off calorimetry [2], [3], [4]. Liquid nitrogen is one of the most abundant inert cryogens, making it relatively safe and affordable to utilize this methodology. However, this technique is limited to the saturation temperature of the fluid. Liquid hydrogen (LH2) stored at 20 K has a high specific energy and the ability to refuel quickly, which is attractive to aviation and freight industries [5]. Understanding the effective conductivities of filler insulations is crucial to the design and sizing of LH2 storage vessels. Utilizing boil-off calorimetry with hydrogen is expensive, introduces safety risks, and is difficult to accumulate sufficient volumes of LH2 for testing. Employing a cryocooler balanced with a guard heater is a known technique that allows for any temperature between 20 and 77 K to be achieved with minimal safety concerns, costs, and complexity, making this an attractive and flexible option for these measurements [6].

In addition to the nominal performance of the insulation, understanding the transient performance during a loss of insulation event is significant in ensuring the proper design and sizing of safety systems. In this study, the design and construction of an effective thermal conductivity test cell capable of taking measurements with a cold boundary temperature of 20 K is accomplished while simultaneously maintaining

the ability to introduce gas into the insulation to simulate a loss of vacuum scenario. A model is developed to determine the theoretical accuracy of the test cell, and preliminary results are reported and compared to existing studies with a cold boundary temperature (CBT) of 77 K in addition to new measurements at 20 K.

## 2. Test cell design

Testing effective thermal conductivities of insulations requires the ability to maintain a temperature differential of approximately 273 K for a CBT of 20 K and a warm boundary temperature (WBT) of 293 K. This is typically done by flowing heat either axially or radially through a cylindrical insulation specimen. Radial heat flow with nested concentric cylinders is most similar to a vacuum-jacketed LH2 storage vessel and chosen for the test-cell geometry. In this study, the internal nested cylinder maintains the warm boundary temperature, the external cylinder maintains the cold boundary temperature via cryocooler, and heat flows radially across the insulation in the annulus. The WBT is maintained via cartridge heater, where the power provided to the heater is the heat flow across the insulation. Equation 1 describes Fourier's law of conduction for this configuration.

$$Q = k_{eff} \frac{2\pi L}{\ln\left(\frac{r_o}{r_i}\right)} \Delta T \tag{1}$$

Where $Q$ is the heater power, k_eff is the effective conductivity, $L$ is the axial length of the insulation, $r_o$ and $r_i$ are the respective external and internal radii of the insulation, and $\Delta T$ is the temperature gradient across the insulation. The test cell needs to be an isolated volume so nitrogen can be introduced without affecting the vacuum chamber pressure, while maintaining gas communication to achieve high vacuum. Figure 1 provides a conceptual diagram of the test cell.

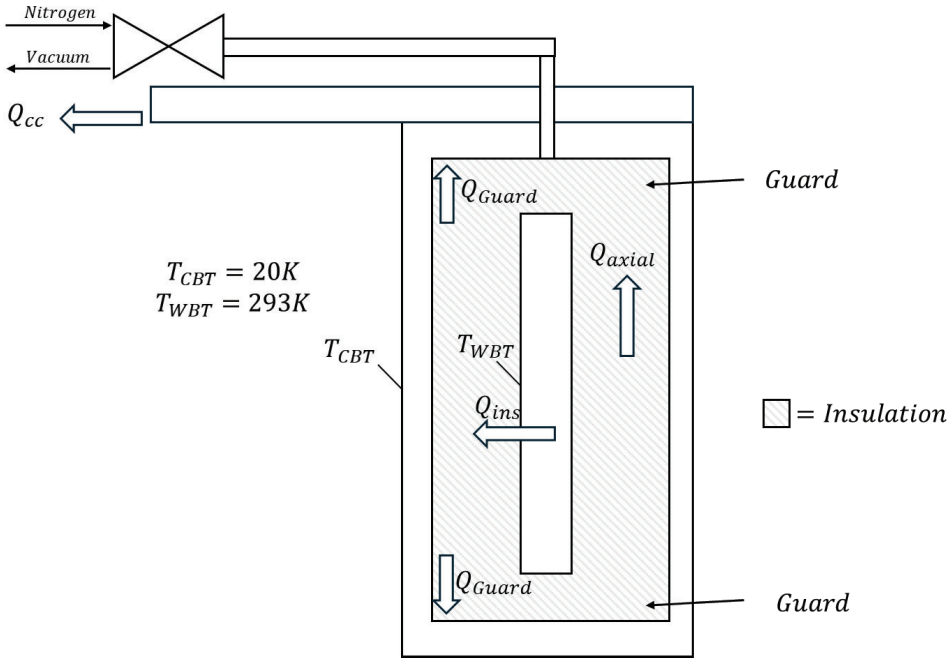


**Figure 1.** Test cell conceptual diagram with heat flows.

The goal when sizing the test cell is to maximize the measured radial heat flow, while minimizing heat flow axially through the insulation and through the guards. Isothermal conditions across the warm and cold

boundary temperatures ensure minimal axial heat flows in the test insulation. Thick guards at the top and bottom of the test cell provide sufficient insulation to further reduce axial heat flows.

In this study, Cryogel Z ™ (Sourced from Aspen Aerogels), CRS 1303 B (Sourced from Lydall), and K1 Glass microbubbles (Sourced from 3M) are the insulations of interest. The aerogel insulation utilized came in a thickness of 10 mm, fixing the annular space of the insulation. The diameter of the internal nested cylinder (heater core) was selected to be 25 mm for machinability and ease of use. To size the remainder of the test cell the length was parametrically varied to minimize the axial to radial heat transfer ratio described in equation 2, while staying in the bounds of the cryocooler's refrigeration power. Where $Q_{guard,total}$ is the combined top and bottom guard heat transfer, and $Q_{ins}$ is the heat transfer through the test insulation. With a 150 mm heater length and 25 mm guard thickness, the axial to radial ratio was approximately 3% in the insulation space. Utilizing a conservative medium vacuum conductivity from previous literature, the heat loads through the insulation and guards are well below the 7 W of cooling that the cryocooler can provide at 20 K.

$$Q_{ax,rad} = \frac{Q_{guard,total}}{Q_{ins}} \tag{2}$$

After preliminary sizing of the test cell, the final materials and geometries are decided upon and used for detailed thermal modeling. Electrolytic tough pitch (ETP) copper was the material of choice for the test cell body and the heater core, given the high thermal conductivity to create nearly isothermal conditions. The heater core needs to be centered in the test cell both axially and radially while simultaneously having the ability to introduce gas into the test cell. Cryogel insulation was utilized both as a guard material and as a means to center the heater core. A hole cut in the top guard allows for gas communication with the heater core. The top flange of the test cell was made from stainless steel to reduce heat losses with the pipe and ensure weldability with the gas communication tube. The top guard is thicker than the bottom to allow the bus bar to interface with the test cell prior to the stainless top flange.

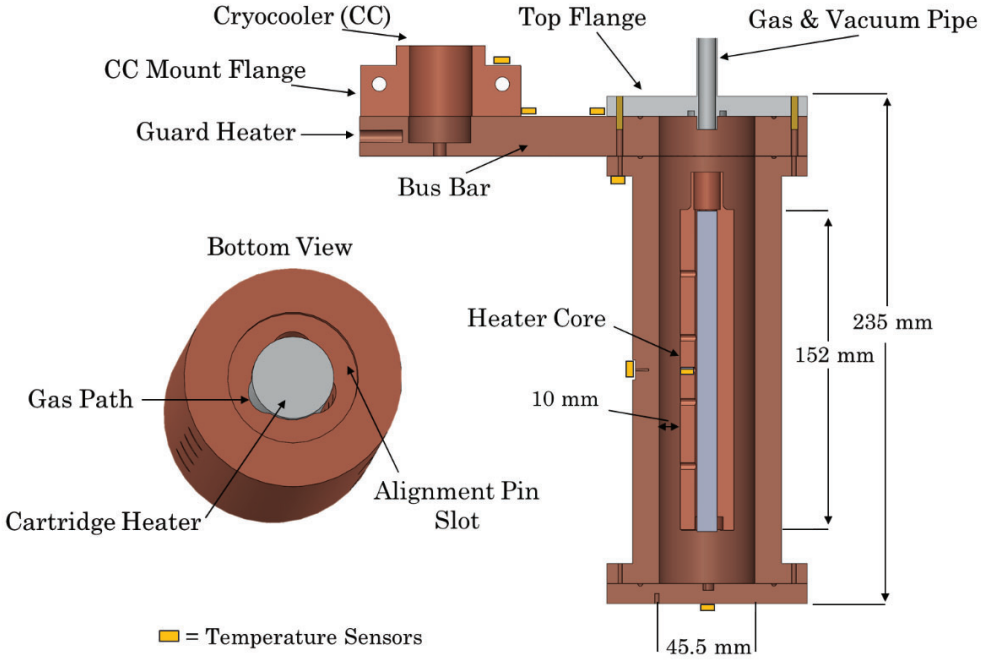


**Figure 2.** Cross-section of the test cell.

The heater core has a cartridge heater at its center that runs the length of the heater core. Three radii 120 degrees apart are milled into the heater core to create gas paths that ensure uniform distribution during a transient event and proper vacuum communication with the entirety of the test cell. Four holes at each set of radii (12 total) were drilled along the length of the heater core into the radii to allow the gas to enter under vacuum or exit during a loss of vacuum event. Figure 2 includes a cross-section of the test cell.

## 3. Thermal model

With materials and geometries identified a thermal resistance network was constructed in which heat is introduced via the heater core and removed at the cryocooler. Resistances through the top and bottom guards as well as radially through the insulation are analytically calculated, and the respective boundary temperatures assigned. The range of possible effective conductivities is parametrically changed to determine the resulting axial to radial heat leak ratio $Q_{ax,rad}$ and total heat load $Q_{total}$. Table 1 summarizes the results of the parametric study.

**Table 1**. Parametric study of test cell heat flows.

| Study | $k_{eff}\left(\frac{mW}{m-K}\right)$ | $Q_{ins}(mW)$ | $Q_{guard,total}(mW)$ | $Q_{total}(mW)$ | $Q_{ax,rad}$ |
|---|---|---|---|---|---|
| 1 | 0.70 | 311 | 12 | 323 | 0.037 |
| 2 | 1.70 | 770 | 46 | 816 | 0.037 |
| 3 | 3.80 | 1690 | 64 | 1754 | 0.037 |
| 4 | 5.86 | 2609 | 98 | 2707 | 0.037 |
| 5 | 7.93 | 3528 | 132 | 3660 | 0.037 |
| 6 | 10.0 | 4447 | 167 | 4614 | 0.037 |

The total heat load from the test cell is well below the 7 W that the cryocooler can provide across all conductivities. The axial-to-radial ratio remains constant because the guards and test insulation will similarly scale conductivities.

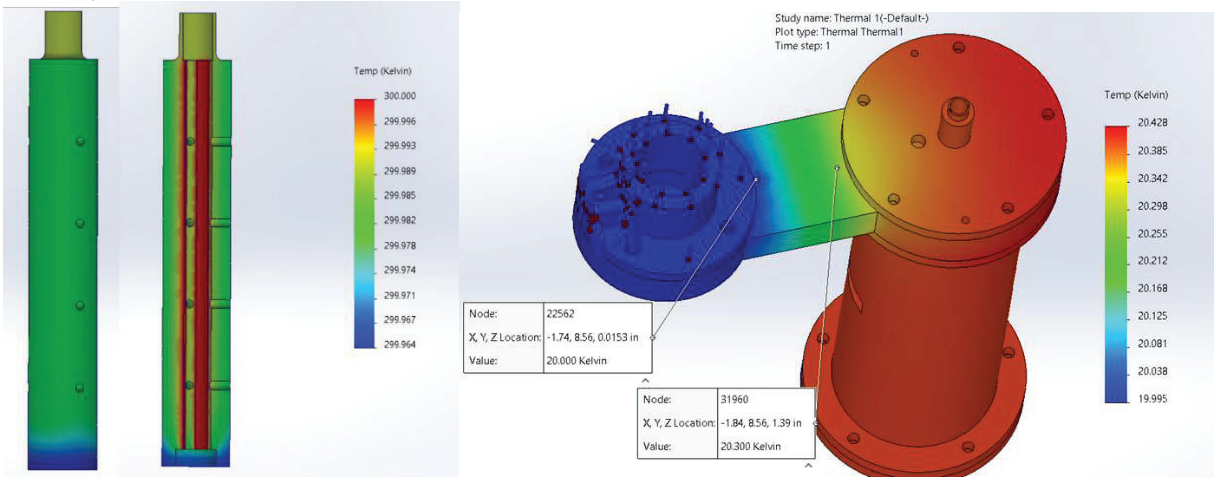


**Figure 3.** Thermal FEA of the heater core (left) and test cell and bus bar assembly (right).

To validate the isothermal conditions of the test cell and heater core a thermal finite element analysis was performed in SOLIDWORKS® 2022. The thermal conductivity of ETP copper at 300 K and 20 K was assigned to the heater core and test cell, respectively [7]. The cryocooler has the ability to remove 7 W at

20 K; applying this heat load as the boundary condition creates the largest delta T. The results of the study are shown in Figure 3. The model shows that for both the heater core and the test cell a maximum delta T of less than 0.2 K is achieved, sufficiently minimizing any non-radial heat transfer. Experimental validation showed the temperature differential was within the 0.5 K accuracy of the silicon diode sensors.

A numerical uncertainty analysis was performed with Engineering Equation Solver (EES) to validate that a measurement accuracy of $\pm\ 1\frac{mW}{m-K}$ could be achieved. The components that contribute to measurement uncertainty are the heater power, uncertainties in geometric conditions, uncertainties in thermal properties, and temperature sensor uncertainties. Table 2 summarizes the resulting uncertainties.

A theoretical uncertainty of $\pm 0.069$ mW/m-K is achieved, putting the system well within the bounds of the $\pm 1$ mW/m-K goal. It is important to mention that the true uncertainty of the system could be higher, and this needs to be verified via repeated testing.

**Table 2.** Uncertainty analysis. $\delta_{\text{offset}}$ is the contribution to uncertainty if the heater core is off-centered by 2 mm. This was calculated via an FEA model in SOLIDWORKS.

| Instrument | Variable $\pm$ Uncertainty | $\%\ of\ uncertainty$ |
|---|---|---|
| Neiko Calipers | $L_{ins} = 152.4 \pm 0.254\ mm$ | 0.13% |
| Neiko Calipers | $R_i = 12.7 \pm 0.254\ mm$ | 56.6% |
| Neiko Calipers | $R_o = 22.8 \pm 0.254\ mm$ | 17.72% |
| Keysight E3642APower Supply | $Q = 538 \pm 5.38\ mW$ | 4.77% |
| Scientific Instruments Silicon diode | $T_{CBT} = 20 \pm 0.5\ K$ | 0.26% |
| Scientific Instruments Silicon diode | $T_{WBT} = 293 \pm 0.5\ K$ | 0.26% |
| - | $\delta_{offset} = 0 \pm 0.0125\frac{1}{m}$ | 20.27% |
| Propagated Uncertainty | $k_{eff} = 1.51 \pm \mathbf{0.069}\frac{\boldsymbol{mW}}{\boldsymbol{m-K}}$ | - |

## 4. Cryostat design

By fixing everything to the lid with a removable lip seal chamber, the internals can be modified with minimal obstruction. The vacuum lid was suspended approximately five feet above the ground via an extruded aluminum frame, allowing the internals to be worked on from a chair. The vacuum chamber has four eyelets welded to the outside for lifting with a cable pulley system and a hand-operated winch. Figure 4 shows the complete assembly. A 32-layer MLI blanket surrounds the internals of the system and is thermally connected to the upper stage of the cryocooler to eliminate thermal radiation as a test variable. Chains fixtured to the lid support the MLI and weight of the test cell, stacked contact resistances between links minimizes conduction heat transfer. The whole system bottoms out with no heat input at 8 K with only 2 W of available refrigeration.


**Figure 4.** Complete assembly of the cryostat.

## 5. Results

Following ASTM C1777-24 Standard Guide for Thermal Performance Testing of Cryogenic Insulation Systems a vacuum bakeout of the insulation is performed at a temperature of 320 K until the vacuum pressure is below 0.1 Pa [6]. Following this, the system is cooled down to the cold boundary temperature at which point a proportional-integral-derivative (PID)-controlled heater maintains the cold side and a DC power supply is adjusted to maintain the WBT. The system is then allowed to steady until the average temperature from minute to minute is nearly identical and the maximum and minimum temperatures over a minute are less than 0.5 K (accuracy of the sensor). This typically takes 1-3 hours.

The emissivity of the heater core was measured to be 0.14 utilizing a FLIR TG 267 infrared camera, then used to calculate the radiation heat transfer present in a vacuum-only measurement. Then the radiation heat transfer was subtracted from the total power supplied to the heater to estimate the axial heat leak through the system guards. This process was repeated twice to account for changes in the wiring connections leading to the heater core that resulted in different parasitic heat loads through the wires. Initial heat leak due to the wires was on the order of 0.5 W. After more thorough insulation of the wires from the cold inlet pipe, this was reduced to 0.1 W. Following ASTM C177-19 Standard Test Method for Steady-State Heat Flux Measurements and Thermal Transmission Properties by Means of the Guarded-Hot-Plate, a bias uncertainty of ± 15% is present after applying the correction given the accuracy and number of previous measurements conducted at 77 K [8].

Table 3 includes the results from the steady state testing with a 20 and 77 K boundary temperature. A plot of the results compared to previous work for the high vacuum scenario is shown in Figure 5. MLI had

the best performance, with microbubbles being the next, followed by vacuum, and lastly, Aerogel. The vacuum measurement is significantly lower than previous measurements. This is due to the low emissivity of the copper test cell, relative to the black sleeve that was utilized to contain filler insulations previously [8], reducing the measured effective conductivity. While the best performance was achieved with MLI, it has a larger value compared to previous measurements. This can be attributed to small-scale, edge effects at the guards and the seam interface of the MLI, resulting in a conservative measurement. Transient testing will be performed following the completion of this testing.

**Table 3**. Summary of steady-state effective conductivities of each insulation. Measurement uncertainty is ±0.069 mW/m-K.

| | **Effective Conductivities** $(\frac{mW}{m-K})$ | | | | |
|---|---|---|---|---|---|
| **Insulation** | $k_{raw\_20\,K}$ | $k_{20\,K}$ *corrected* | $k_{raw\_77\,K}$ | $k_{77\,K}$ *corrected* | $CVP\ (mPa)$ |
| Vacuum | 1.20 | 0.85 | 1.53 | 1.07 | 5.8 |
| Aerogel | 2.45 | 0.95 | 2.91 | 1.31 | 3.2 |
| Glass Microbubbles | 0.87 | 0.52 | 1.02 | 0.56 | 2.9 |
| MLI (2 layers/mm) | 0.62 | 0.26 | 0.76 | 0.30 | 3.1 |

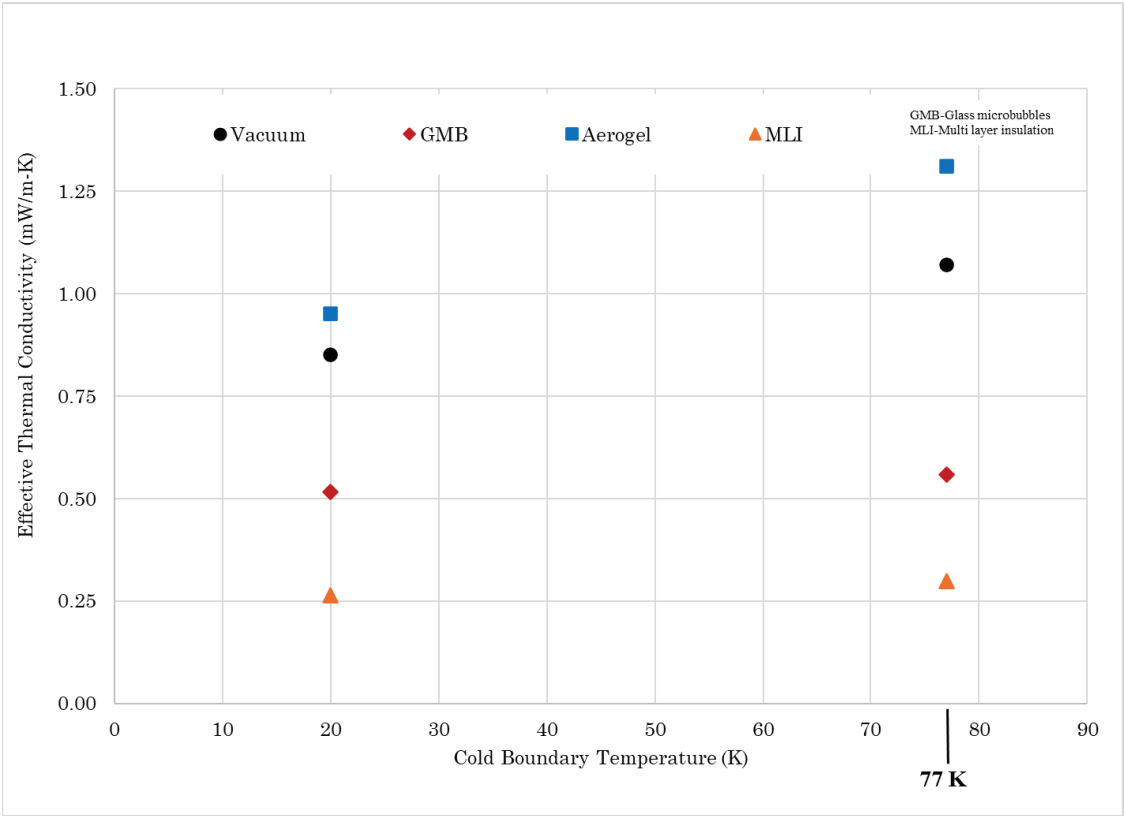


**Figure 5.** Corrected effective conductivity at high vacuum <0.013 Pa at a warm boundary temperature of 293 K.

## 6. Conclusions

A test apparatus for characterizing insulations at liquid hydrogen boundary temperatures has been developed. Aerogel, Glass Microbubbles, Multi-Layer insulation, and Vacuum were tested under high vacuum (<0.013 Pa) at a warm boundary temperature of 293 K and cold boundary temperatures of 77 and 20 K. The collected measurements have a theoretical uncertainty of $\pm$ 0.069 mW/m-K. Preliminary results indicate a lower than previously reported vacuum conductivity at 77 K, Aerogel and Microbubbles are within 15% of previous measurements, and MLI is approximately 0.2 mW/m-K higher than previous measurements. The lowest conductivity was measured with MLI, followed by glass microbubbles, vacuum, and aerogel. Across all insulations, going from 77 K to 20 K resulted in a drop in effective conductivity, with aerogel experiencing the largest drop of 27%. Future testing will be performed on each of the insulations during a transient loss of vacuum event to characterize heat flux.

### Acknowledgements

These results have been established in collaboration with Airbus

### References

[1] Hydrogen Tools, “Liquid Storage Vessels.” Accessed: Apr. 10, 2025. [Online]. Available: https://h2tools.org/bestpractices/hydrogen-system-components/liquid-storage-vessels
[2] J. E. Fesmire and W. L. Johnson, “Thermal Performance Data for Multilayer Insulation Systems Tested between 293 K and 77 K,” 2015.
[3] J. E. Fesmire and S. D. Augustynowicz, “Thermal Performance Testing of Glass Microspheres under Cryogenic Vacuum Conditions,” in AIP Conference Proceedings, American Institute of Physics Inc., Jun. 2004, pp. 612–618. doi: 10.1063/1.1774734.
[4] B. E. Coffman, J. E. Fesmire, S. White, G. Gould, and S. Augustynowicz, “Aerogel blanket insulation materials for cryogenic applications,” in AIP Conference Proceedings, 2010, pp. 913–920. doi: 10.1063/1.3422458.
[5] Department of Energy, “Hydrogen Storage.” Accessed: Apr. 10, 2025. [Online]. Available: https://www.energy.gov/eere/fuelcells/hydrogen-storage
[6] “Guide for Thermal Performance Testing of Cryogenic Insulation Systems,” Mar. 15, 2024, ASTM International, West Conshohocken, PA. doi: 10.1520/C1774-24.
[7] NIST, “Material Properties: OFHC Copper (UNS C10100/C10200).” Accessed: Apr. 10, 2025. [Online]. Available: https://trc.nist.gov/cryogenics/materials/OFHC%20Copper/OFHC_Copper_rev1.htm
[8] J. Ekins, Experimental techniques for low-temperature measurements: cryostat design, material properties and superconductor critical-current testing. Oxford university press, 2006.